



Design, synthesis and structure–activity relationship studies of morpholino-1*H*-phenalene derivatives that antagonize Mcl-1/Bcl-2



Xiangqian Li^{a,b}, Xiaomeng Liang^a, Ting Song^a, Pengchen Su^a, Zhichao Zhang^{a,*}

^aState Key Laboratory of Fine Chemicals, School of Chemistry, Dalian University of Technology, Dalian, China

^bOcean University of China, 238 Songling Road, Qingdao, China

ARTICLE INFO

Article history:

Received 14 May 2014

Revised 19 September 2014

Accepted 23 September 2014

Available online 2 October 2014

Keywords:

Dual inhibitors

Hydrogen bond

Apoptosis

Mcl-1

Bcl-2

ABSTRACT

We report herein characteristic studies of Mcl-1 and Bcl-2 dual inhibitors. It was found that a protruding carbonyl group forming hydrogen bond with R263 plays a predominant role compared with the hydrophobic group that occupies the p2 pocket. A series of dual inhibitors representing different parts of the morpholino-1*H*-phenalene were designed, synthesized and evaluated.

© 2014 Elsevier Ltd. All rights reserved.

1. Introduction

The programmed cell death (apoptosis) machinery follows several well-organized cell signaling networks where one of the two major pathways (i.e., the mitochondrial process or intrinsic pathway) involves a highly regulated series of proteins.^{1–3} As the central regulators of this pathway, Bcl-2 family members contain from one to four Bcl-2 homology (BH) domains and can be broadly divided into two classes: anti-apoptotic and pro-apoptotic proteins.^{4,5} A balance between these two classes dictates a cell's fate and is mediated by the BH3 domain of the BH3-only proteins inserting into a hydrophobic groove on the surface of anti-apoptotic proteins including Bcl-2, Bcl-xL, and Mcl-1.⁶

Overexpression of anti-apoptotic Bcl-2 family proteins occurs in many human cancers, and therefore, these proteins are very attractive targets for the development of novel anticancer agents.^{7,8} One of the most promising inhibitors to date is ABT-737 which inhibits multiple members of the prosurvival proteins of the Bcl-2 family except for Mcl-1.^{9,10} Accordingly, it is a poor killer of most cells, except those that have reduced Mcl-1 levels, or in which Mcl-1 degradation has been induced.¹¹ As such, a potent small-molecule inhibitor of Bcl-2 family proteins should bind not only to Bcl-2 and Bcl-xL, but also to Mcl-1 with high affinities.^{12,13}

Mcl-1 plays a notable pro-survival role in vivo, and its elimination in response to cytotoxic signals is critical in promoting

cell death.^{14–17} However, it has been identified that the BH3 groove of Mcl-1 is different with that of Bcl-2.^{18,19} Although some molecules reported are capable to bind to both Mcl-1 and Bcl-2,^{7,20,21} it is rarely discussed the key features for a dual inhibitor. The design of Mcl-1/Bcl-2 dual inhibitor is still a challenge.

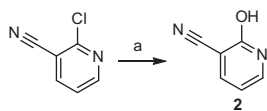
Previously, we reported a small-molecule Mcl-1/Bcl-2 dual inhibitor, 3-thiomorpholin-8-oxo-8*H*-acenaphtho[1,2-*b*]pyrrole-9-carbonitrile (**1**).^{22,23} The binding mode of **1** with Bcl-2/Mcl-1 has been illustrated by structure–activity relationship study. Based on its structural information, we designed some novel dual inhibitors not only to provide more candidates for clinical development, but also to reveal the crucial parts of compound **1**. Guided by our discovery, more potent Mcl-1/Bcl-2 dual inhibitors could be designed and synthesized.

2. Chemistry

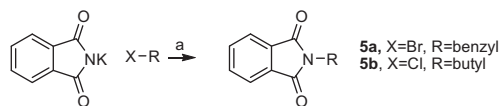
Compounds **2** and **2b** were prepared according to the method that we reported previously (Schemes 1 and 2).²⁴ The synthetic route of the 5-(phenylthio)isoindoline-1,3-dione derivatives (**4a**, **4b**, **4d**, and **4f**) was outlined in Scheme 3.^{25,26} 4-Bromophthalic acid was prepared by bromination of phthalic anhydride, and it was converted to 4-bromophthalimide as a white crystalline powder by dehydration and imidization. The target compounds were obtained by the reaction between 4-bromophthalimide and corresponding thiophenol with K₂CO₃ at 130 °C in DMF. The syntheses of **4c**, **4e**, **4g**, and **4h** were accomplished by the reaction of

* Corresponding author. Tel./fax: +86 411 84986032.

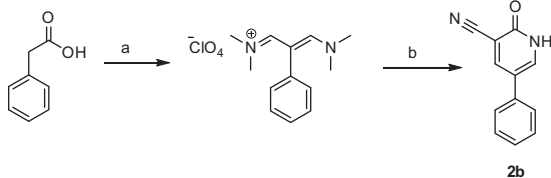
E-mail address: zc Zhang@dlut.edu.cn (Z. Zhang).



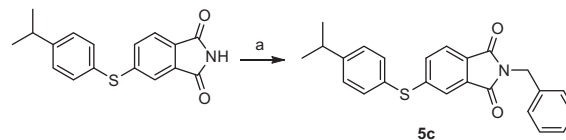
Scheme 1. Synthesis of **2**. Reagents and conditions: (a) CH_3COOH , 120°C , 8 h.



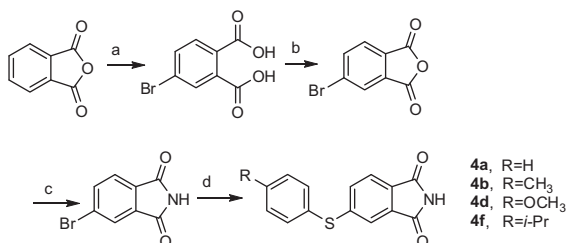
Scheme 5. Synthesis of **5a** and **5b**. Reagents and conditions: (a) DMF, 70°C , 2 h.



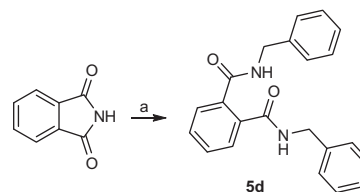
Scheme 2. Synthesis of **2b**. Reagents and conditions: (a) DMF, POCl_3 , 80°C , 3 h; H_2O , NaClO_4 ; (b) NaOMe , MeOH , $\text{NCCH}_2\text{CONH}_2$, rt 2 h; reflux, 3 h; H_2O .



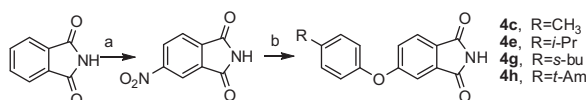
Scheme 6. Synthesis of **5c**. Reagents and conditions: (a) benzyl bromide, DMF, K_2CO_3 , 70°C , 30 min.



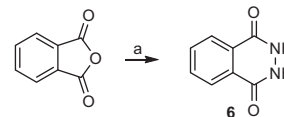
Scheme 3. Synthesis of **4a**, **4b**, **4d** and **4f**. Reagents and conditions: (a) NaOH , H_2O , Br_2 , 90°C , 6 h; HCl ; (b) Ac_2O , 140°C , 2 h; (c) $\text{CO}(\text{NH}_2)_2$, 160°C , 1 h; (d) 4-R-PhSH, K_2CO_3 , CuI , DMF, 130°C , N_2 , 6 h.



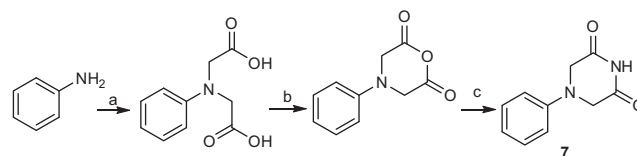
Scheme 7. Synthesis of **5d**. Reagents and conditions: (a) benzylamine, DMF, K_2CO_3 , 50°C , 2 h.



Scheme 4. Synthesis of **4c**, **4e**, **4g** and **4h**. Reagents and conditions: (a) HNO_3 , H_2SO_4 , 3 h; (b) 4-R-PhOH, K_2CO_3 , CuI , DMF, 130°C , N_2 , 18–30 h.



Scheme 8. Synthesis of **6**. Reagents and conditions: (a) $\text{N}_2\text{H}_4 \cdot \text{H}_2\text{O}$, $\text{C}_2\text{H}_5\text{OH}$, reflux, 1 h.



Scheme 9. Synthesis of **7**. Reagents and conditions: (a) ClCH_2COOH , KOH , H_2O , 70°C , 4 h; HCl ; (b) Ac_2O , 140°C , 2 h; (c) $\text{CO}(\text{NH}_2)_2$, 110°C , 1 h.

corresponding phenol with 4-nitrophthalimide with K_2CO_3 at 130°C in DMF (Scheme 4).

Compounds **5a–5c** were synthesized according to Gabriel synthesis (Schemes 5 and 6). Compound **5d** was prepared by the reaction of phthalimide and benzylamine with K_2CO_3 at 50°C in DMF (Scheme 7).²⁷ Compound **6** was obtained by the reaction of phthalic anhydride and hydrazine hydrate in ethanol under reflux for 1 h (Scheme 8).²⁸ Compound **7** was synthesized according to the route described in Scheme 9, and the starting material phenylamine was converted to **7** by three steps, substitution, dehydration and imidization.²⁹

3. Results and discussion

Our previous studies revealed that compound **1** is able to form a hydrogen bond with Arg263 in Mcl-1 through its carbonyl group, while the thiomorpholine inserts into the p2 pocket of Mcl-1 (Fig. 1a).²³ The structural information suggested that not only the hydrogen bonding but also hydrophobic interactions contribute to the dual inhibition of Mcl-1 and Bcl-2. Here, we intended to explore the significance of these two kinds of mimicking for the Mcl-1/Bcl-2 dual inhibitors.

Firstly, **1** was deconstructed into small pieces **2** and **3** (Fig. 2 and Scheme 1). The binding affinities (K_i) of these compounds were

evaluated using Fluorescence polarization assay (FPA) (Fig. 3a, and b). The commerce thiomorpholine **3** could not bind to Mcl-1 at all, while **2** exhibited a weak affinity ($K_i = 17.9 \mu\text{M}$). Consequently, two compounds (**2a**, **2b**) were obtained by introducing a benzene ring to enrich the complexity of **2**. Although, the structure of these two compounds, **2a** and **2b**, is very different from compound **1**, the effective carbonyl group that may form a hydrogen bond with Arg263 was still reserved (Fig. 2, Scheme 2).

FPA showed **2a** binds to Mcl-1 and Bcl-2 with K_i values of $6.9 \mu\text{M}$ and $11.6 \mu\text{M}$, respectively, while **2b** binds to Mcl-1 with a K_i value of $9.51 \mu\text{M}$, but shows no appreciable binding to Bcl-2 (Table 1, Fig. 3a and b). Relatively high affinity of these two simply fragments implies that all that is required for ligand-Arg263 interaction is an amide. The predicted binding model showed that one of carbonyl groups in **2a** forms a hydrogen bond with Arg263 in Mcl-1 (Fig. 1b). Therefore, compound **2a** was selected as a starting point for the further optimization.

Based on our predicted binding model for **2a**, we designed and synthesized a series of 5-substituted compounds, **4a–4h**, using

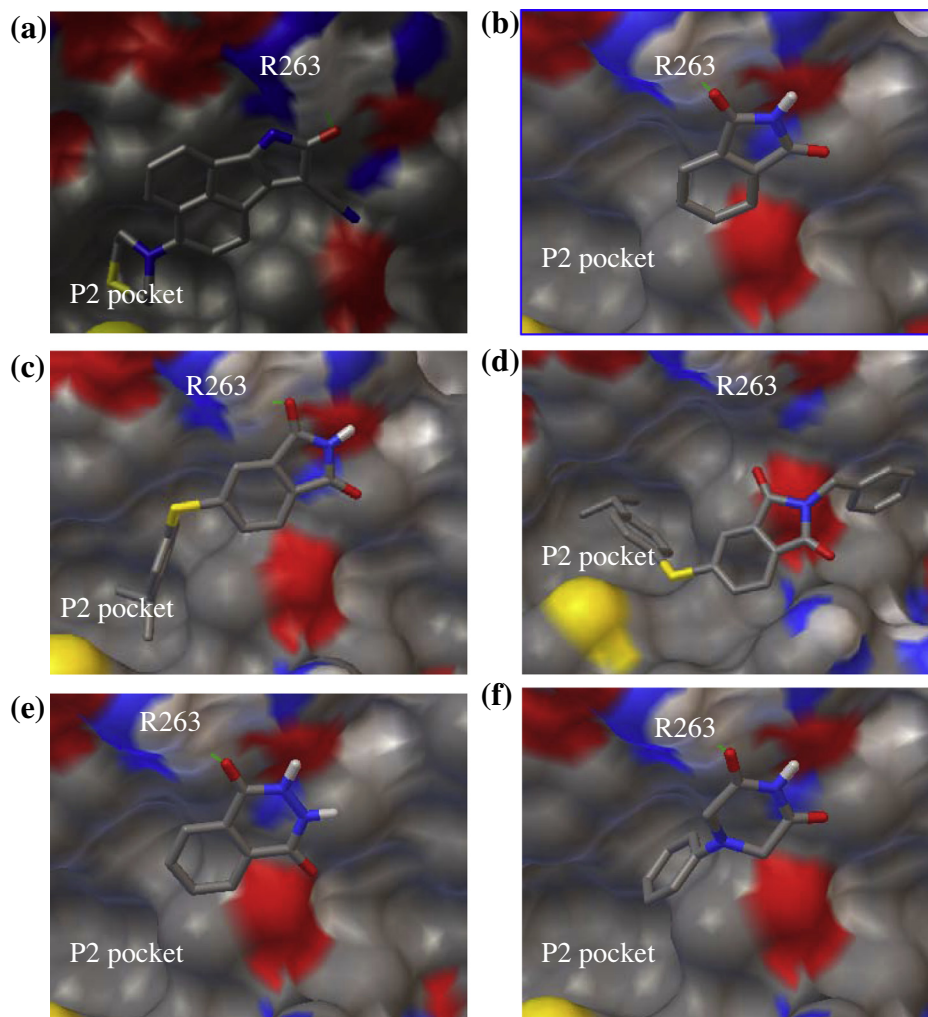


Figure 1. Predicted binding models of Mcl-1 in complex with (a) **1**, (b) **4f**, (c) **4h**, (d) **5c**, (e) **6** and (f) **7**. Carbon, hydrogen, oxygen, nitrogen, and sulfur atoms in all designed compounds and in surface of Mcl-1 are in gray, white, red, blue, and yellow, respectively. Hydrogen bonds are depicted as dashed lines in green.

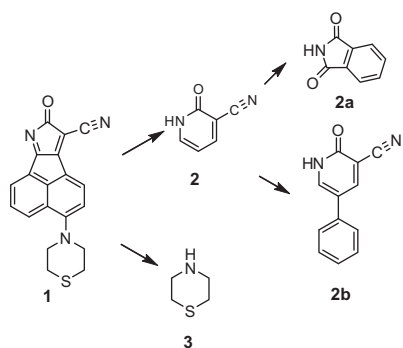


Figure 2. Deconstruction of **1** into fragments by maintaining key groups (highlighted in red).

benzenethiol, 4-methylbenzenethiol, 4-methylphenol, 4-methoxybenzenethiol, 4-isopropylphenol, 4-isopropylbenzenethiol, 4-*sec*-butylphenol, and 4-*tert*-pentylphenol as the substituent groups (Schemes 3 and 4). In our previous SAR studies, we successfully occupied the p2 pocket of Mcl-1/Bcl-2 by using these groups.²³ Very similar to the survey of these substituent groups in the previous study, progressive increase in steric bulk of the group resulted in the corresponding increase in binding affinity, and overlarge

substituent group resulted in no binding (Fig. 3a and b, and Table 1). The most potent compound **4f** binds to Mcl-1 and Bcl-2 with K_i values of 298 nM and 1.1 μ M, respectively. **4h** showed no binding.

Analysis of the predicted binding models showed the isopropyl of **4f** can mimic the iso-butyl group of Leu62 in the Bim BH3 peptide to fill the p2 pocket of Mcl-1, while one of the carbonyl groups forms a hydrogen bond with Arg263. As shown in Figure 1b, the position and orientation of **4f** in the BH3 groove is very similar to that of **1**. 4-*tert*-amylphenoxy of **4h**, however, cannot be accommodated well inside the p2 pocket because of steric hindrance (Fig. 1c). Comparing to **1**, the **4** series compounds hold the very different structure but the similar binding mode and affinity. Compounds **4f** and **1** shared the same carbonyl group and similar hydrophobic groups, both of which are proposed to contribute to the binding.

To further identify the direct binding ability of **4f** and **4h** to Mcl-1, isothermal titration calorimetry (ITC) was performed (Fig. 4a and b). In consistent with their K_i values showed in Table 1, **4f** exhibited a K_d value of 0.632 μ M, illustrating the binding to Mcl-1, while **4h** shows no appreciable binding to Mcl-1, presumably due to the added steric bulk of the neopentyl group. It further confirmed that forming hydrogen bond with R263 plays the most important role in binding to Mcl-1.

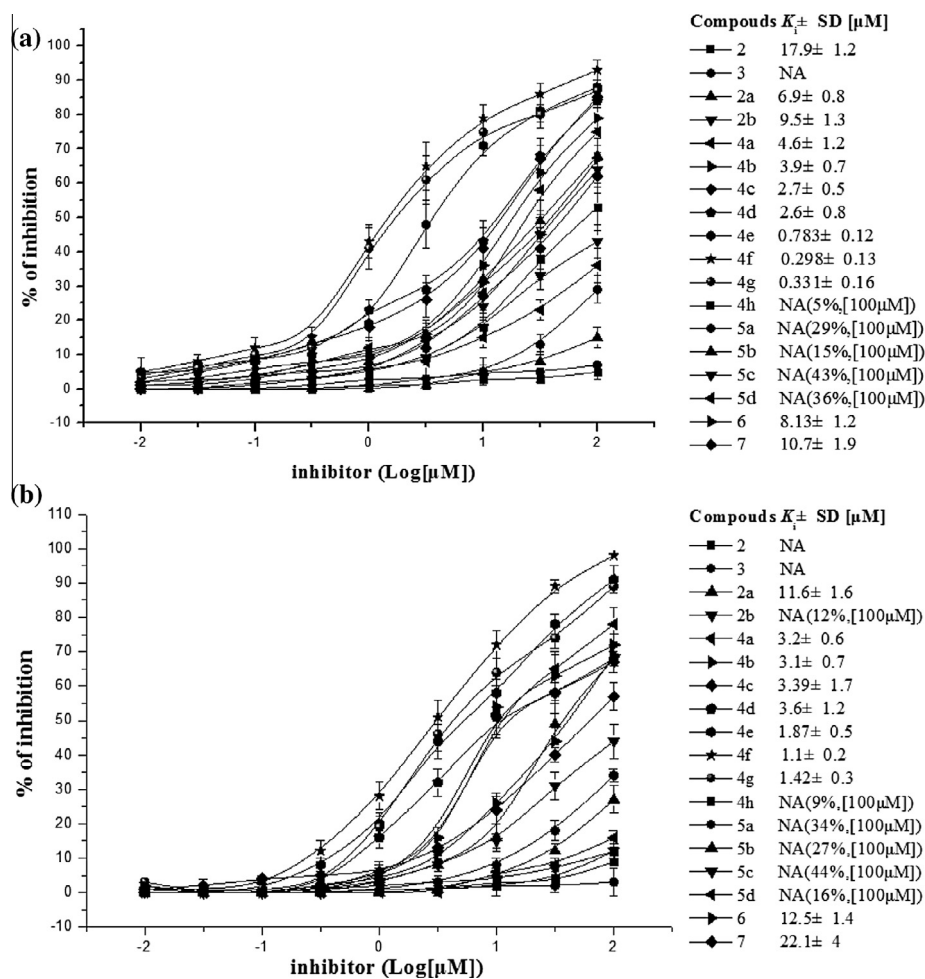


Figure 3. Competitive binding curves of designed compounds to (a) Mcl-1 and (b) Bcl-2 proteins as determined using a fluorescence-polarization assay.

We tried to explore the striking feature of the carbonyl group for the binding of these compounds to the targets. Firstly, we found the carbonyl group protrudes from the molecular platform. We then referred to the three dimension structure of Bim in a complex with Mcl-1 (Fig. 5a and b). We found that the Arg263 is surrounded by four residues, Val253, Asp256, Val258 and Asn260. Arg263 is flush with these four residues. Accordingly, Asp67 in Bim that forms salt bridge with Arg263 protrudes from the backbone of the peptide (Fig. 5b). As such, we hypothesized that an exposed hydrogen-bond donor should be a specific feature for **1** and the **4** series as a dual inhibitor. Consequently, we referred to the pan-Bcl-2 inhibitors TW-37 and TM-179.^{20,30} These compounds also hold a protruding pyrogallol group, which forms hydrogen bond with Arg263 in Mcl-1 and Arg146 in Bcl-2.

Encouraged by the above findings, we designed compounds **5a–5d** to further verify that a protruding hydrogen-bond donor plays a critical role in this binding model. Three groups of different sizes were introduced to *N*-position of **2a** and **4f** (Schemes 5–7). Our FP-based binding assay determined that these four compounds showed no appreciable binding to Mcl-1 or Bcl-2 at the concentration as high as 100 μM (Fig. 3a and b). As expected, the docking study showed that **5c** lost the hydrogen bond with Arg263 of Mcl-1 (Fig. 1d). It illustrated that a hydrogen-bond donor protruding from the molecular platform should be necessary for the formation of the hydrogen bond in this binding model. When a steric hindrance is available, either the big rigid substituent groups such as the phenyl and benzyl of **5a**, **5c** and **5d**, or the small

flexibility substituent such as the butyl of **5b**, could hampered the hydrogen bond.

From the predicted binding model, we found **5c** could still occupy the P2 pocket, though it loses the hydrogen bond (Fig. 1d). Additionally, the single hydrophobic group itself, such as compound **3**, did not show any affinity, while compound **2** which held a six-ring as simple as thiomorpholine showed a weak but appreciable binding. These data indicated that the carbonyl group may play a more important role in this binding model than the hydrophobic groups. This result is inconsistent with the Bim BH3 alanine mutations reported by W. Douglas Fairlie.¹⁸ The D67A mutant which destroyed the interaction with Arg263 had significant effects on Mcl-1 binding, but no significant effects were observed with L62A mutant which occupied p2 pocket in Mcl-1.

In order to further confirm that Arg263 in Mcl-1 (Arg146 in Bcl-2) plays a predominant role for dual inhibitors to capture, other two compounds **6** and **7** were designed and synthesized (Schemes 8 and 9). On the premise of maintaining the protruding carbonyl group, the crucial part of **6** binding to Arg263 becomes a stable six-membered ring, while that of **7** becomes a flexible ring. FP-based binding assays showed that compound **6** has K_i of 8.13 μM and 12.5 μM to Mcl-1 and Bcl-2, respectively, while **7** was determined to bind to Mcl-1 and Bcl-2 with K_i values of 10.7 μM and 22.1 μM , respectively. Although the structures of these two compounds have changed a lot compared with **1**, both of them still maintain the dual inhibition of Mcl-1 and Bcl-2. The protruding hydrogen bond donor in the proper position is the determinant.

Table 1
Structure and binding affinities of small-molecule inhibitors to Mcl-1 and Bcl-2 as determined by FPAs

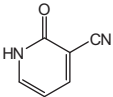
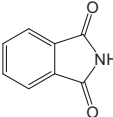
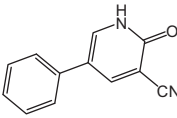
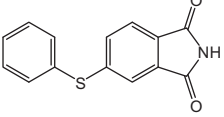
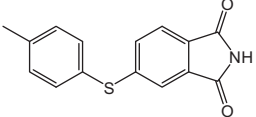
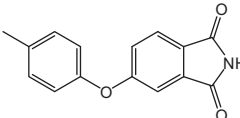
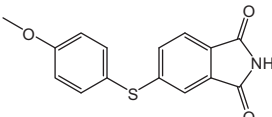
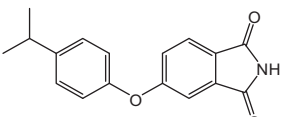
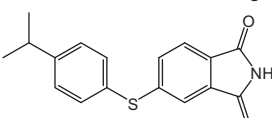
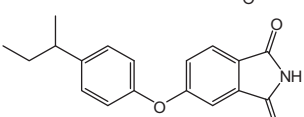
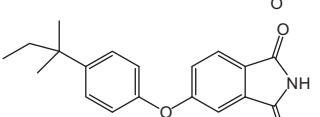
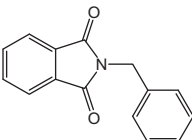
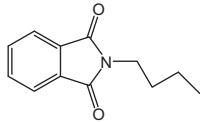
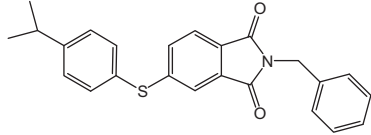
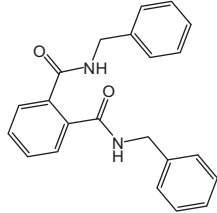
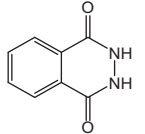
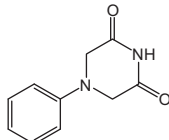
Compounds	Structure	K_i^a (Mcl-1)	K_i^a (Bcl-2)
2		17.9 μ M	NA
3		NA	NA
2a		6.9 \pm 0.8 μ M	11.6 \pm 1.6 μ M
2b		9.5 \pm 1.3 μ M	12%, [100 μ M]
4a		4.6 \pm 1.2 μ M	3.2 \pm 0.6 μ M
4b		3.69 \pm 0.7 μ M	3.1 \pm 0.7 μ M
4c		2.7 \pm 0.5 μ M	3.39 \pm 1.7 μ M
4d		2.63 \pm 0.8 μ M	3.6 \pm 1.2 μ M
4e		783 \pm 120 nM	1.87 \pm 0.5 μ M
4f		298 \pm 130 nM	1.1 \pm 0.2 μ M
4g		331 \pm 160 nM	1.42 \pm 0.3 μ M
4h		5%, [100 μ M]	9%, [100 μ M]
5a		29%, [100 μ M]	34%, [100 μ M]

Table 1 (continued)

Compounds	Structure	K_i^a (Mcl-1)	K_i^a (Bcl-2)
5b		15%, [100 μ M]	27%, [100 μ M]
5c		43%, [100 μ M]	44%, [100 μ M]
5d		36%, [100 μ M]	16%, [100 μ M]
6		$8.13 \pm 1.2 \mu$ M	$12.49 \pm 1.4 \mu$ M
7		$10.7 \pm 1.9 \mu$ M	$22.1 \pm 4 \mu$ M

^a Values were measured by FPA for inhibition constant (K_i). The values are the mean \pm SD of three independent experiments.

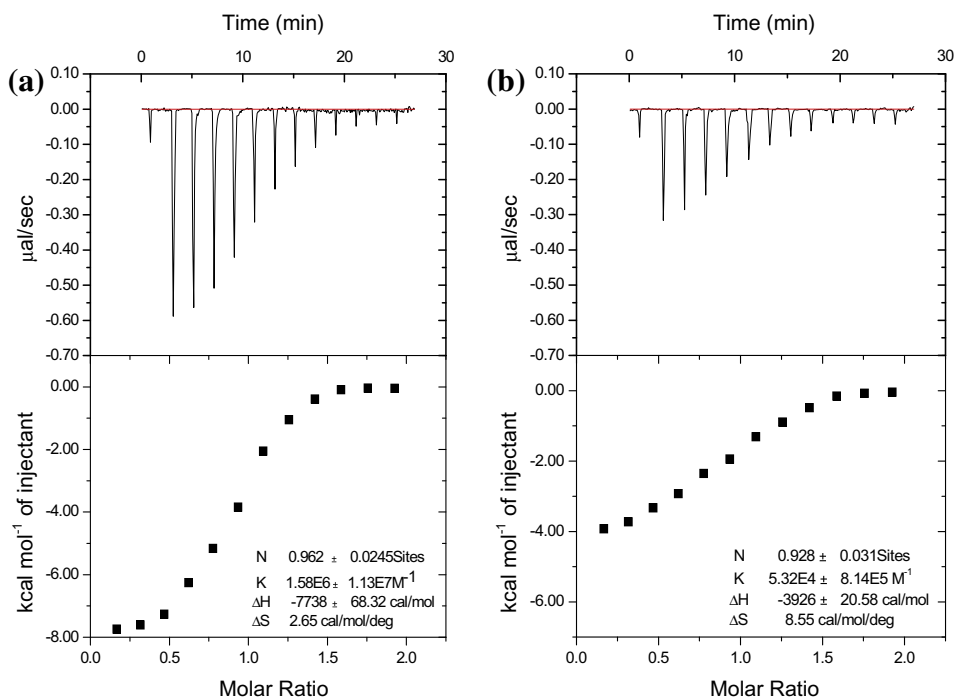


Figure 4. The binding affinities determined by ITC of (a) **4f** and (b) **4h** to Mcl-1, respectively. The upper panels display the raw titration data. Each point on the curves in the lower panels represent.

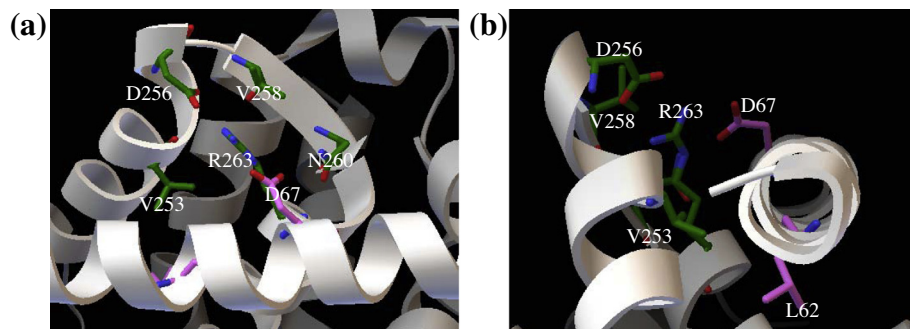


Figure 5. Positions of residues around R263 in a Ribbon diagram of the Bim/Mcl-1 complex (a) front view, (b) side view.

Analysis of the binding model of **6** and **7** to Mcl-1 (Fig. 1e and f) confirmed that one of the carbonyls of them can form hydrogen bond with Arg263 in Mcl-1.

4. Conclusions

In summary, our study demonstrates although both Arg263 (Arg146 in Bcl-2) and p2 pocket are the hotspots of Mcl-1 and Bcl-2, the Arg263 in Mcl-1 (Arg146 in Bcl-2) shows the predominant requirement for the dual inhibitors to capture. The appropriate hydrogen bonding donors need to protrude from the molecular platform, while isopropyl and sec-butyl shows proper size and hydrophobic property to occupy the p2 pocket. The molecules that well occupy both of these two sites could gain good dual inhibition.

5. Experimental section

5.1. Materials and methods

All commercial reagents were purchased and used without further purification or distillation unless otherwise stated. ^1H NMR was obtained with Bruker AV-400 spectrometer with chemical shifts reported as ppm (in CDCl_3 , TMS as internal standard). The following abbreviations are used for multiplicity of NMR signals: s = singlet, d = doublet, t = triplet, q = quartet, m = multiplet, br = broad. High-resolution mass spectra (HRMS) were obtained on HPLC-Q-ToF MS (Micro) spectrometer. Column chromatography was performed on silica gel 200–300 mesh. Purity of all final products was determined by analytical HPLC to be $\geq 95\%$. HPLC purity of compounds was measured with a normal phase HPLC (XBridge C18, 4.6×150 mm, $5 \mu\text{M}$) with two diverse wavelength detection systems.

5.2. Synthesis

5.2.1. 2-Hydroxynicotinonitrile (**2**)

Acetic acid (20 mL) was added in three portions to 2-chloronicotinonitrile (1.38 g, 10 mmol) under stirring at room temperature. Then, the temperature raised to 120°C , and kept for 8 h. After cooled to room temperature, the resulting precipitation was filtered. 2-hydroxynicotinonitrile was obtained as white needle crystal.

Yield: 68%, ^1H NMR (400 MHz, CDCl_3): δ : 10.12 (s, 1H), 7.93 (d, $J = 8.0$ Hz, 1H), 7.72 (d, $J = 8.0$ Hz, 1H), 6.34 (m, 1H). TOF MS (EI^+): $\text{C}_6\text{H}_4\text{N}_2\text{O}$, found 121.03. Mp: $224\text{--}225^\circ\text{C}$.

5.2.2. 5-Phenyl-2-hydroxynicotinonitrile (**2b**)

A mixture of dimethylformamide (1.96 g, 27 mmol) and phosphoryl chloride (2.47 g, 16 mmol) and 2-phenylacetic acid

(734 mg, 5.4 mmol) was stirred for 3 h at 80°C . The mixture was put on ice (30 g) and conc. NaClO_4 solution was added. The resulting precipitate was filtered off and washed with diluted NaClO_4 solution. The product was used in the next step without further disposal.

The solid was added to a solution of sodium methoxide (0.162 g, 3.0 mmol) in 13 mL of CH_3OH . Then cyanoacetamide (0.10 g, 3.28 mmol) was added. The mixture was stirred for 2 h and then refluxed 3 h during which time a yellow solid separated. Water was added, and the mixture was acidified and filtered to remove a yellow solid which was washed with water, ethanol, ether, and then hexane to give crude product. The crude product was recrystallized from ethanol.

Yield: 392 mg, 61%. ^1H NMR (400 MHz, CDCl_3): δ : 12.97 (s, 1H), 8.30 (s, 1H), 8.02 (s, 1H, Ar-H), 7.49–7.52 (d, $J = 8.0$ Hz, 2H), 7.41–7.43 (m, 3H). TOF MS (EI^+): $\text{C}_{12}\text{H}_8\text{N}_2\text{O}$, found 196.06. Mp: $232\text{--}233^\circ\text{C}$.

5.2.3. General procedure for the preparation of **4a**, **4b**, **4d** and **4f**

To sodium hydroxide (2.4 g, 0.06 mol) dissolved in water (20 mL) was added phthalic anhydride (4.44 g, 0.03 mol). When complete solution was obtained, bromine (9.4 g, 3 mL, 0.06 mol) was incrementally added, while stirring, over 1 h. The reaction mixture was heated to 90°C and allowed to react under reflux for 6 h. After standing for 10 h, the white solids that crystallized out of solution were filtered, washed with cold water, and analyzed as monosodium 4-bromophthalic acid salt. The total product was dissolved in hot water, and the pH was adjusted to about 1.5 by addition of concentrated hydrochloric acid. The resulting solution was evaporated to dryness on a rotary evaporator and extracted with acetone to give 4-bromophthalic acid. Yield: 5.0 g, 68%, mp: $164\text{--}166^\circ\text{C}$.

A solution of 4-bromophthalic acid (5 g, 0.02 mol) and acetic anhydride (30 mL) was heated for 2 h at 140°C . The reaction mixture was cooled to room temperature and the excess of acetic anhydride was removed under reduced pressure. The residue was washed with petroleum ether and then 4-bromophthalic anhydride was obtained as white solid. Yield: 3.8 g, 84%, mp: $104\text{--}106^\circ\text{C}$.

4-Bromophthalic anhydride (2.26 g, 0.01 mol) was added to urea (6.0 g, 0.1 mol). Then the solid mixture was heated till molten, and maintained at 160°C for 2 h. After cooled, the solid was washed with 100 mL water and recrystallized with ethanol (100 mL). 4-Bromophthalimide was obtained as white solid. Yield: 1.32 g, 58%, mp: $230\text{--}233^\circ\text{C}$.

The mixture of 4-bromophthalimide (225 mg, 1 mmol), 4-R-PhSH (3 mmol), K_2CO_3 (136 mg, 1 mmol) and CuI (10 mg) was added to DMF (10 mL). The solution was heated at 130°C for 6 h under the protection of nitrogen. After cooled, water (30 mL) was added and the precipitation was filtered, washed with water. The

product was purified by column chromatography on silica gel using dichloromethane/acetone (60:1).

5.2.3.1. 5-(Phenylthio)isoindoline-1,3-dione (4a). Yield: 85 mg, 38%. $^1\text{H NMR}$ (400 MHz, CDCl_3): δ 7.92 (s, 1H, NH), 7.69 (d, $J = 8.0$ Hz, 1H), 7.52 (q, $J = 8.0$ Hz, 2H), 7.50 (d, $J = 8.0$ Hz, 1H), 7.46 (m, 4H). TOF MS (EI^+): $\text{C}_{14}\text{H}_9\text{NO}_2\text{S}$, found 255.03. Mp: 169–171 °C.

5.2.3.2. 5-(*p*-Tolylthio)isoindoline-1,3-dione (4b). Yield: 140 mg, 52%. $^1\text{H NMR}$ (400 MHz, CDCl_3): δ 7.79 (s, 1H, NH), 7.66 (d, $J = 8.0$ Hz, 1H), 7.43 (m, 4H), 7.27 (d, $J = 8.0$ Hz, 2H), 2.42 (s, 3H). TOF MS (EI^+): $\text{C}_{15}\text{H}_{11}\text{NO}_2\text{S}$, found 269.05. Mp: 154–156 °C.

5.2.3.3. 5-(4-Methoxyphenylthio)isoindoline-1,3-dione (4d). Yield: 121 mg, 42%. $^1\text{H NMR}$ (400 MHz, CDCl_3): δ 7.91 (s, 1H, NH), 7.66 (d, $J = 8.0$ Hz, 1H), 7.48 (d, $J = 8.0$ Hz, 2H), 7.38 (m, 2H), 6.99 (d, $J = 8.0$ Hz, 2H), 3.87 (s, 3H). TOF MS (EI^+): $\text{C}_{15}\text{H}_{11}\text{NO}_3\text{S}$, found 285.05. Mp: 157–159 °C.

5.2.3.4. 5-(4-Isopropylphenylthio)isoindoline-1,3-dione (4f). Yield: 110 mg, 37%. $^1\text{H NMR}$ (400 MHz, CDCl_3): δ 8.09 (s, 1H, NH), 7.67 (d, $J = 8.0$ Hz, 1H), 7.48 (m, 4H), 7.32 (d, $J = 8.0$ Hz, 2H), 2.96 (m, 1H), 1.29 (d, $J = 4.0$ Hz, 6H). TOF MS (EI^+): $\text{C}_{17}\text{H}_{15}\text{NO}_2\text{S}$, found 297.08. Mp: 151–152 °C.

5.2.4. General procedure for the preparation of 4c, 4e, 4g and 4h

To a stirred, cold (ice-bath) solution of 22 mL of fuming aqueous nitric acid and 50 mL of concentrated aqueous sulfuric acid was added, portionwise, 14.7 g (0.1 mol) of phthalimide. The mixture was allowed to warm to room temperature. After about 3 h, complete solution was obtained. The yellow solution was slowly poured, with stirring, onto 200 g ice. The crude product which precipitated was collected by filtration and 4-nitrophthalimide was recrystallized from ethanol to afford 8.74 g (45.5%) as yellow solid. Mp: 198–202 °C.

The mixture of 4-nitrophthalimide (192 mg, 1 mmol), 4-R-PhOH (3 mmol), K_2CO_3 (136 mg, 1 mmol) and CuI (10 mg) was added to DMF (10 mL). The solution was heated at 130 °C for 18–30 h under the protection of nitrogen. After cooled, water (30 mL) was added and the precipitation was filtered, washed with water. The product was purified by column chromatography on silica gel using dichloromethane/acetone (60:1).

5.2.4.1. 5-(*p*-Tolyloxy)isoindoline-1,3-dione (4c). Yield: 104 mg, 41%. $^1\text{H NMR}$ (400 MHz, CDCl_3): δ 7.70 (s, 1H, NH), 7.27 (m, 2H), 7.21 (m, 2H), 6.97 (m, 2H), 6.74 (d, $J = 8.0$ Hz, 1H), 2.38 (s, 3H). TOF MS (EI^+): $\text{C}_{15}\text{H}_{11}\text{NO}_3$, found 253.07. Mp: 161–162 °C.

5.2.4.2. 5-(4-Isopropylphenoxy)isoindoline-1,3-dione (4e). Yield: 50 mg, 18%. $^1\text{H NMR}$ (400 MHz, CDCl_3): δ 7.80 (s, 1H), 7.59 (s, 1H, NH), 7.52 (d, $J = 8.0$ Hz, 1H), 7.43 (d, $J = 8.0$ Hz, 1H), 7.36 (d, $J = 8.0$ Hz, 2H), 7.06 (d, $J = 8.0$ Hz, 2H), 2.91 (m, 1H), 1.27 (d, $J = 8.0$ Hz, 6H). TOF MS (EI^+): $\text{C}_{17}\text{H}_{15}\text{NO}_3$, found 282.06. Mp: 157–159 °C.

5.2.4.3. 5-(4-*sec*-Butylphenoxy)isoindoline-1,3-dione (4g). Yield: 193 mg, 62%. $^1\text{H NMR}$ (400 MHz, CDCl_3): δ 7.79 (d, $J = 8.0$ Hz, 1H), 7.69 (s, 1H, NH), 7.30 (m, 2H), 7.24 (m, 2H), 7.01 (d, $J = 4.0$ Hz, 2H), 2.64 (m, 1H), 1.62 (m, 2H), 1.27 (d, $J = 4.0$ Hz, 3H), 0.85 (t, $J = 8.0$ Hz, 3H). TOF MS (EI^+): $\text{C}_{18}\text{H}_{17}\text{NO}_2\text{S}$, found 295.12. Mp: 146–147 °C.

5.2.4.4. 5-(4-*tert*-Pentylphenoxy)isoindoline-1,3-dione (4h). Yield: 40 mg, 13%. $^1\text{H NMR}$ (400 MHz, CDCl_3): δ 7.88 (s, 1H, NH), 7.79 (d, $J = 4.0$ Hz, 1H), 7.37 (d, $J = 4.0$ Hz, 2H), 7.28 (m, 2H), 7.01

(d, $J = 4.0$ Hz, 2H), 1.67 (m, 2H), 1.31 (s, 6H), 0.73 (t, $J = 8.0$ Hz, 3H). TOF MS (EI^+): $\text{C}_{19}\text{H}_{19}\text{NO}_3$, found 309.13. Mp: 140–142 °C.

5.2.5. General procedure for the preparation of 5a and 5b

A mixture of phthalimide potassium (500 mg, 2.7 mmol), and benzyl bromide or 1-butyl chloride (6.0 mmol) was stirred in DMF (10 mL) for 2 h at 70 °C. After cooled to room temperature, the solution was poured into 20 mL cooled water, stirred for 10 h. The precipitation was filtered, washed with water and recrystallized with ethanol/ H_2O (20 mL/20 mL).

5.2.5.1. 2-Benzylisoindoline-1,3-dione (5a). Yield: 300 mg, 46%, white needle crystal. $^1\text{H NMR}$ (400 MHz, CDCl_3): δ 7.83 (m, 2H), 7.68 (m, 2H), 7.31 (d, $J = 4.0$ Hz, 2H), 7.27 (d, $J = 8.0$ Hz, 1H), 7.24 (s, 1H), 4.84 (s, 2H, CH_2). TOF MS (EI^+): $\text{C}_{15}\text{H}_{11}\text{NO}_2$, found 237.08. Mp: 117–118 °C.

5.2.5.2. 2-Butylisoindoline-1,3-dione (5b). Yield: 155 mg, 28%, white solid. $^1\text{H NMR}$ (400 MHz, CDCl_3): δ 7.84 (m, $J = 8.0$ Hz, 2H), 7.71 (m, $J = 8.0$ Hz, 2H), 3.69 (t, 2H, CH_2), 1.66 (m, 2H, CH_2), 1.38 (m, 2H, CH_2), 0.95 (t, 3H, CH_3). TOF MS (EI^+): $\text{C}_{12}\text{H}_{13}\text{NO}_2$, found 203.09. Mp: 33–35 °C.

5.2.6. 2-Benzyl-5-(4-isopropylphenylthio)isoindoline-1,3-dione (5c)

A mixture of 5-(4-isopropylphenylthio)isoindoline-1,3-dione (4f) (148 mg, 0.5 mmol), benzyl bromide (171 mg, 1.0 mmol), and K_2CO_3 (136 mg, 1.0 mmol) was stirred in DMF (10 mL) for 30 min at 70 °C. After cooled to room temperature, the solution was poured into 20 mL cooled water and extracted with ethyl acetate. The resulting product was purified by column chromatography on silica gel using ethyl acetate/petroleum ether (1:20) as the mobile phase.

Yield: 118 mg, 60%, white solid. $^1\text{H NMR}$ (400 MHz, CDCl_3): δ 7.66 (d, $J = 8.0$ Hz, 1H), 7.48–7.40 (m, 5H), 7.30–7.27 (m, 4H), 7.24 (d, $J = 8.0$ Hz, 1H), 4.80 (d, $J = 4.0$ Hz, 2H, CH_2), 2.95 (m, 1H), 1.28 (d, $J = 4.0$ Hz, 6H). TOF MS (EI^+): $\text{C}_{24}\text{H}_{21}\text{NO}_2\text{S}$, found 387.13. Mp: 94–96 °C.

5.2.7. *N*¹,*N*²-Dibenzylphthalimide (5d)

A mixture of phthalimide (147 mg, 1.0 mmol), benzylamine (321 mg, 3.0 mmol), and K_2CO_3 (136 mg, 1.0 mmol) was stirred in DMF (10 mL) for 2 h at 50 °C. After cooled to room temperature, the solution was poured into 20 mL cooled water. The resulting precipitate was filtered, washed with water.

Yield: 267 mg, 77%, white solid. $^1\text{H NMR}$ (400 MHz, CDCl_3): δ 7.60 (d, $J = 8.0$ Hz, 2H), 7.45 (d, $J = 8.0$ Hz, 2H), 7.35–7.28 (m, 10H), 6.96 (s, 2H), 4.51 (d, $J = 4.0$ Hz, 4 H). TOF MS (EI^+): $\text{C}_{22}\text{H}_{20}\text{N}_2\text{O}_2$, found 344.14. Mp: 174 – 177 °C.

5.2.8. 2,3-Dihydrophthalazine-1,4-dione (6)

Phthalic anhydride (1.48 g, 10 mmol) was dissolved in ethanol (20 mL), then to this mixture was added hydrazine hydrate (2 mL, 50%, 20 mmol) dropwise. The reaction mixture was refluxed 1 h. After cooled to room temperature, the white solid was collected through filtration.

Yield: 1.32 g, 82%, white solid. $^1\text{H NMR}$ (400 MHz, CDCl_3): δ 11.52 (s, 2H), 8.10 (m, 2H), 7.90 (m, 2H). TOF MS (EI^+): $\text{C}_8\text{H}_6\text{N}_2\text{O}_2$, found 161.04. Mp: >300 °C.

5.2.9. 4-Phenylpiperazine-2,6-dione (7)

A mixture of phenylamine (186 mg, 2 mmol), 2-chloroacetic acid (470 mg, 5 mmol) and KOH (560 mg, 10 mmol) was stirred in H_2O (20 mL) for 4 h at 70 °C. After being cooled down, the mixture was adjusted to acidic with 0.1 N HCl. The precipitate was collected by suction filtration, washed with cold water and dried. Yield: 263 mg, 63%.

A solution of 2,2'-(phenylazanediy)diacetic acid (418 mg, 2 mmol) and acetic anhydride (10 mL) was heated for 2 h at 140 °C. The reaction mixture was cooled to room temperature and the excess of acetic anhydride was removed under reduced pressure. The residue was used in the next step without further disposal.

The residue (4-phenylmorpholine-2,6-dione) was added to urea (1.8 g, 30 mmol), then, the solid mixture was heated till molten. The molten reaction was stirred for 1 h at 110 °C and cooled. Acetic ether (20 mL) was added. The organic layer was washed with brine and dried with MgSO₄. Concentration of the organic layer afforded the desired crude product. After evaporation under reduced pressure, the product was purified by column chromatography on silica gel using dichloromethane/acetone (60:1).

Yield: 0.167 mg, 44%. ¹H NMR (400 MHz, CDCl₃): δ 8.32 (s, 1H), 7.33 (t, J = 12.0 Hz, 2H), 7.02 (t, J = 8.0 Hz, 1H), 6.35 (d, J = 4.0 Hz, 2H), 4.10 (s, 4H). TOF MS (EI⁺): C₁₀H₁₀N₂O₂, found 190.07. Mp: 157–158 °C.

5.3. Binding affinity assay

5.3.1. Regents, plasmid and antibodies

A 21-residue Bid BH3 peptide (residues 79–99) bearing a 6-carboxyfluorescein succinimidyl ester fluorescence tag (FAM-Bid) was synthesized at HD Biosciences (Shanghai, China). Recombinant human Bcl-2 protein was purchased from Santa Cruz Biotechnology (sc-4096, Santa Cruz). Caspase colorimetric protease assay kit was purchased from Keygen Biotech (KGA202, Keygen, China). pEGFP-C1/Mcl-1 plasmid and pET28a(+)/Mcl-1 plasmid were constructed in our Lab. Lipofectamine™ 2000 Transfection Reagent was from Invitrogen (11668-500, invitrogen). Antibodies were Bcl-2 antibody (sc-783, Santa Cruz) and rabbit antibody against Mcl-1 (BS1220, Bioworld).

5.3.2. Fluorescence polarization-based binding assay (FPA)

For the competitive binding assay for Bcl-2 protein, FAM-Bid peptide (10 nM) and Bcl-2 protein (200 nM) were preincubated in the assay buffer (25 mM Tris, pH 8.0; 150 mM NaCl). Next, serial dilutions of compounds were added. After a 30-min incubation, the polarization values were measured using the Spectra Max M5 Detection System in a black 96-well plate. Saturation experiments determined that FAM-Bid binds to the Bcl-2 protein with a K_d value of 112 nM. For Mcl-1, assays were performed in the same manner as that for Bcl-2 with the following exceptions: 50 nM Mcl-1 and 10 nM FAM-Bid peptide were used in the assay buffer. FAM-Bid peptide binds to the Mcl-1 protein with a K_d value of 13 nM.

5.3.3. Isothermal titration calorimetry (ITC) assay

Isothermal titration calorimetry (ITC) was performed using ITC200 (Microcal). Experiments were performed in 20 μM Tris pH 8.0, 150 mM NaCl, 1% DMSO at 25 °C. For evaluating K_d value of compounds, titrations consisted of 12 × 3 μL injections of compound at 300 μM into Mcl-1 (30 μM). All sample data obtained after control data corrections were analyzed to fit to a one-site model. For control ITC experiments, the sample cells were filled with assay buffer and the compound solution was added. This process was identical to that for protein samples.

5.4. Molecular docking

The 3D structures of the human Mcl-1 (hMcl-1; PDB ID: 2NLA) and human Bcl-2 (Bcl-2; PDB ID: 1GJH) were obtained from the

protein bank in the RCSB. The 3D structures of the inhibitors were generated using ChemBio3D Ultra 11.0 followed by energy minimization. AutoDock 4.0 program equipped with ADT was used to perform the automated molecular docking.

Acknowledgments

The work was supported by the National Natural Science Foundation of China (21372036, 81272876, 81430083, 21402022).

Supplementary data

Supplementary data associated with this article can be found, in the online version, at <http://dx.doi.org/10.1016/j.bmc.2014.09.047>.

References and notes

- Fesik, S. W. *Nat. Rev. Cancer* **2005**, *5*, 876.
- Mukherjee, P.; Desai, P.; Zhou, Y.-D.; Avery, M. J. *Chem. Inf. Model.* **2010**, *50*, 906.
- Brunelle, J. K.; Ryan, J.; Yecies, D.; Opferman, J. T.; Letai, A. J. *Cell Biol.* **2009**, *187*, 429.
- Hu, X.; Sun, J.; Wang, H.-G.; Manetsch, R. J. *Am. Chem. Soc.* **2008**, *130*, 13820.
- Vogler, M.; Dinsdale, D.; Dyer, M. J.; Cohen, G. M. *Cell Death Differ.* **2008**, *16*, 360.
- Cory, S.; Huang, D. C.; Adams, J. M. *Oncogene* **2003**, *22*, 8590.
- Wei, J.; Kitada, S.; Rega, M. F.; Stebbins, J. L.; Zhai, D.; Cellitti, J.; Yuan, H.; Emdadi, A.; Dahl, R.; Zhang, Z. *J. Med. Chem.* **2009**, *52*, 4511.
- Degterev, A.; Boyce, M.; Yuan, J. *J. Cell Biol.* **2001**, *155*, 695.
- Oltersdorf, T.; Elmore, S. W.; Shoemaker, A. R.; Armstrong, R. C.; Augeri, D. J.; Belli, B. A.; Bruncko, M.; Deckwerth, T. L.; Dinges, J.; Hajduk, P. J. *Nature* **2005**, *435*, 677.
- van Delft, M. F.; Wei, A. H.; Mason, K. D.; Vandenberg, C. J.; Chen, L.; Czabotar, P. E.; Willis, S. N.; Scott, C. L.; Day, C. L.; Cory, S. *Cancer Cell* **2006**, *10*, 389.
- Lee, E.; Czabotar, P.; Smith, B.; Deshayes, K.; Zobel, K.; Colman, P.; Fairlie, W. *Cell Death Differ.* **2007**, *14*, 1711.
- Azmi, A. S.; Mohammad, R. M. *J. Cell. Physiol.* **2009**, *218*, 13.
- Kitada, S.; Leone, M.; Sareth, S.; Zhai, D.; Reed, J. C.; Pellecchia, M. J. *Med. Chem.* **2003**, *46*, 4259.
- Willis, S. N.; Chen, L.; Dewson, G.; Wei, A.; Naik, E.; Fletcher, J. I.; Adams, J. M.; Huang, D. C. *Genes Dev.* **2005**, *19*, 1294.
- Lin, X.; Morgan-Lappe, S.; Huang, X.; Li, L.; Zakula, D.; Vernetti, L.; Fesik, S.; Shen, Y. *Oncogene* **2006**, *26*, 3972.
- Brunelle, J. K.; Shroff, E. H.; Perlman, H.; Strasser, A.; Moraes, C. T.; Flavell, R. A.; Daniel, N. N.; Keith, B.; Thompson, C. B.; Chandel, N. S. *Mol. Cell Biol.* **2007**, *27*, 1222.
- Huang, H.-M.; Huang, C.-J.; Yen, J. J.-Y. *Blood* **2000**, *96*, 1764.
- Lee, E. F.; Czabotar, P. E.; Van Delft, M. F.; Michalak, E. M.; Boyle, M. J.; Willis, S. N.; Puthalakath, H.; Bouillet, P.; Colman, P. M.; Huang, D. C. *J. Cell Biol.* **2008**, *180*, 341.
- Zhang, Z.; Yang, H.; Wu, G.; Li, Z.; Song, T.; Li, X. Q. *Eur. J. Med. Chem.* **2011**, *46*, 3909.
- Wang, G.; Nikolovska-Coleska, Z.; Yang, C.-Y.; Wang, R.; Tang, G.; Guo, J.; Shangary, S.; Qiu, S.; Gao, W.; Yang, D. *J. Med. Chem.* **2006**, *49*, 6139.
- Nguyen, M.; Marcellus, R. C.; Roulston, A.; Watson, M.; Serfass, L.; Madiraju, S. M.; Goulet, D.; Viallet, J.; Bélec, L.; Billot, X. *Proc. Natl. Acad. Sci.* **2007**, *104*, 19512.
- Zhang, Z.; Jin, L.; Qian, X.; Wei, M.; Wang, Y.; Wang, J.; Yang, Y.; Xu, Q.; Xu, Y.; Liu, F. *ChemBioChem* **2007**, *8*, 113.
- Zhang, Z.; Wu, G.; Xie, F.; Song, T.; Chang, X. *J. Med. Chem.* **2011**, *54*, 1101.
- Zhang, Z.; Liu, C.; Li, X.; Song, T.; Liang, X.; Zhao, Y.; Shen, X.; Chen, H. *Eur. J. Med. Chem.* **2012**, *60*, 410.
- Lin, M.-J.; Wang, J.-D.; Chen, N.-S.; Huang, J.-L. *J. Coord. Chem.* **2006**, *59*, 607.
- Cocoman, M. K.; Schwartz, W.T. Process for the preparation of 4-bromophthalic anhydride, EP Patent 0429040, 1991.
- Sheikh, C.; Takagi, S.; Ogasawara, A.; Ohira, M.; Miyatake, R.; Abe, H.; Yoshimura, T.; Morita, H. *Tetrahedron* **2010**, *66*, 2132.
- Prime, M. E.; Courtney, S. M.; Brookfield, F. A.; Marston, R. W.; Walker, V.; Warne, J.; Boyd, A. E.; Kairies, N. A.; von der Saal, W.; Limberg, A. *J. Med. Chem.* **2010**, *54*, 312.
- Zhang, Y.; Huang, Y.; Huang, C. C. *J. Labelled Compd. Radiopharm.* **2005**, *48*, 485.
- Tang, G.; Nikolovska-Coleska, Z.; Qiu, S.; Yang, C.-Y.; Guo, J.; Wang, S. *J. Med. Chem.* **2008**, *51*, 717.